



ELSEVIER

Contents lists available at ScienceDirect

Comput. Methods Appl. Mech. Engrg.

journal homepage: www.elsevier.com/locate/cma

Generalized variability response functions for two-dimensional elasticity problems

Kirubel Teferra ^{a,*}, Sanjay R. Arwade ^b, George Deodatis ^c^a Weidlinger Associates, New York, NY 10005, USA^b Dept. of Civil and Environmental Engg., University of Massachusetts, Amherst, MA 01002, USA^c Dept. of Civil Engg. & Engg. Mechanics, Columbia University, New York, NY 10027, USA

ARTICLE INFO

Article history:

Received 14 May 2013

Received in revised form 9 January 2014

Accepted 12 January 2014

Available online 23 January 2014

Keywords:

Uncertainty quantification

Effective properties

Random fields

Variability response functions

ABSTRACT

The ability to determine probabilistic characteristics of response quantities in structural mechanics (e.g. displacements, stresses) as well as effective material properties is restricted due to lack of information on the probabilistic characteristics of the uncertain system parameters. The concept of the variability response function (VRF) has been proposed as a means to systematically capture the effect of the stochastic spectral characteristics of uncertain system parameters modeled by homogeneous random fields on the uncertain structural response. The key property of the VRF in its classical sense is its independence from the marginal probability distribution function (PDF) and the spectral density function (SDF) of the uncertain system parameters (it depends only on the deterministic structural configuration and boundary conditions). Proofs have been provided for the existence of VRFs for linear and some nonlinear statically determinate beams. For statically indeterminate structures, the Monte Carlo based generalized variability response function (GVRF) methodology has been proposed recently as a generalization of the VRF concept to indeterminate linear and some nonlinear beams. The methodology computes GVRFs, which are analogous to VRFs for statically determinate structures, and evaluates their dependence (or lack thereof) on the PDF and SDF of the random field, thereby providing an estimate of the accuracy of the GVRF. In this paper, the GVRF methodology is extended to problems involving two-dimensional, linear continua whose stochasticity is characterized by statistically homogeneous random fields. After detailing the GVRF methodology for two-dimensional random fields, two numerical examples are provided: GVRFs are computed for the displacement response and for the effective compliance of linear plane stress systems.

© 2014 Elsevier B.V. All rights reserved.

1. Introduction

The difficulty in establishing probabilistic characterizations of the response stochasticity of structures with uncertain system parameters (e.g. material properties) arises from the computational effort required to solve such problems and the challenges in developing realistic, detailed models for system parameter stochasticity (a lack of data, an inability to measure the desired parameters, model error, noisy measurements, and many more factors). An efficient way to address this problem is to establish functions providing probabilistic information of a response quantity of a structure while being independent of the uncertain parameters. Such functions allow efficient computation, and by virtue of their independence from the system

* Corresponding author. Tel.: +1 (212) 367 2825.

E-mail address: kt377@columbia.edu (K. Teferra).

parameters, allow stochastic sensitivity analysis of the system. One such function is the variability response function (VRF), first proposed by Shinozuka [24], which is essentially a Green's function relating the variance of a response quantity of a structure (e.g. displacement) to the spectral density function (SDF) of the uncertain system parameters. In the VRF approach, it is assumed that the uncertain system can be described by a homogeneous random field, $f(\mathbf{x})$. With the exception of a few problems involving approximate Taylor expansion techniques [6,7,19,31], the VRF in previous literature is established for problems where the homogeneous random field is a one-dimensional function $f(x)$. However, in general three-dimensional problems, an expression for the variance of a displacement quantity $u(\mathbf{x})$ is sought as

$$\text{Var}[u(\mathbf{x})] = \int_{\Omega_{\mathbf{k}}} \text{VRF}_u(\mathbf{x}, \boldsymbol{\kappa}) S_f(\boldsymbol{\kappa}) d\boldsymbol{\kappa}, \quad (1)$$

where $S_f(\boldsymbol{\kappa})$ is the SDF of the zero-mean, homogeneous random field $f(\mathbf{x})$ modeling the uncertain system parameters, $\boldsymbol{\kappa} = (\kappa_1, \kappa_2, \kappa_3)$ is the wavenumber, and $\mathbf{x} = (x_1, x_2, x_3)$ is the spatial location. The function $\text{VRF}_u(\mathbf{x}, \boldsymbol{\kappa})$ is a deterministic function that depends on deterministic properties of the structure, loading, and boundary conditions. It identifies the sensitivity of the response variability to the spectral characteristics (or equivalently the correlation structure) of $f(\mathbf{x})$ and provides the supremum of the response variance if only the variance of $f(\mathbf{x})$ is known (i.e. this is where $S_f(\boldsymbol{\kappa}) = \frac{\sigma_f^2}{2} [\delta(\boldsymbol{\kappa} - \boldsymbol{\kappa}^*) + \delta(\boldsymbol{\kappa} + \boldsymbol{\kappa}^*)]$ with $\text{VRF}_u(\mathbf{x}, \boldsymbol{\kappa}^*)$ being the maximum value of $\text{VRF}_u(\mathbf{x}, \boldsymbol{\kappa})$). For analytically derived expressions for the exact VRF for the displacement response of statically determinate beams, the reader is referred to Refs. [1,5] for linear constitutive laws and Ref. [28] for nonlinear constitutive laws. Ref. [23] provides exact analytical expressions for the VRF for the effective flexibility (\bar{D}) of statically determinate beams. In this case, the variance of \bar{D} is expressed as

$$\text{Var}[\bar{D}] = \int_{-\infty}^{\infty} \text{VRF}_{\bar{D}}(\kappa) S_f(\kappa) d\kappa. \quad (2)$$

A computationally efficient numerical approach called the Fast Monte Carlo methodology, first proposed in [25] and further developed in [20,21], can be applied to general linear finite element systems to establish an approximate VRF for statically indeterminate structures. This method involves a fundamental conjecture: a unique VRF exists for statically indeterminate structures that is independent of the PDF and SDF of the random field modeling the uncertain system parameters. However, it is known that exact expressions for the VRF for statically indeterminate structures do not exist because the response variance cannot be expressed as a function that is separable with respect to its deterministic component and a function associated with the spectral content of the random field. Thus, a methodology has been proposed as an improvement to the Fast Monte Carlo methodology whose aim is to establish a generalized VRF (GVRF) for linear, statically indeterminate structures while evaluating the potential dependence of the computed GVRFs on the random field [18]. The degree of dependence, which can be quantified by the GVRF method, is directly related to the degree of approximation that occurs when equations such as Eqs. (1) and (2) are applied to indeterminate structures.

In the GVRF methodology, the uncertain system parameters are described by random fields having a wide range of combinations of marginal PDFs and SDFs. For each combination considered, a corresponding GVRF is computed. If all the computed GVRFs are approximately the same, then the GVRFs can be assumed to be nearly independent of the random fields, and the GVRFs can be utilized analogously to the classical VRF.

The applicability of the GVRF methodology has been demonstrated for the displacement response of linear indeterminate beams [18], a class of nonlinear indeterminate beams [28], and for the effective flexibility of linear indeterminate beams [27]. These problems involve one-dimensional random fields. In this paper, the GVRF methodology is extended to include linear continua whose stochasticity is modeled by two-dimensional random fields (e.g. elastic modulus of plane stress/strain structures). The numerical examples considered are the GVRF for the response displacement of a plane stress structure and the GVRF for the effective compliance of a plane stress structure. The paper is outlined as follows: the VRF concept related to the homogenization of material properties is described in Section 2. The GVRF methodology is detailed for two-dimensional stochastic problems in Section 3 and the numerical examples mentioned above follow in Section 4. The paper concludes with a discussion of the results.

2. VRF concept for effective material properties

Homogenization of material properties into effective properties occurs, often implicitly, when conducting standard tests such as tensile tests, direct shear tests, v-notch tests, creep tests, and others. This is because most materials exhibit random heterogeneity at the meso- and micro-scales. It is shown in [22] that elastic effective properties can be considered as deterministic when the structure considered is sufficiently larger than the correlation length scale of the uncertain heterogeneities. The size of the structure where the effective properties become effectively deterministic corresponds to that of the representative volume element (RVE). When the structure considered is smaller than the RVE, the effective properties are random variables [2,8,11,13,16,32]. The development of multiscale finite element analysis has provided a means of propagating material property uncertainty across scales [12,14,29]. A need exists, however, for efficient methods based on sound mechanics that provide a direct connection between material property uncertainty at different scales.

Consider a heterogeneous body Ω described by coordinates $\mathbf{x} \in \mathbb{R}^3$ whose material properties can be described as locally isotropic. The strong form of the boundary value problem with its boundary conditions is

$$\boldsymbol{\sigma}_{ij,j} + \mathbf{b}_i = 0 \quad (3a)$$

$$\boldsymbol{\sigma}_{ij} = \mathbf{C}_{ijkl}(\mathbf{x}) \boldsymbol{\epsilon}_{kl} \quad (3b)$$

$$\boldsymbol{\epsilon}_{ij} = \frac{1}{2}(\mathbf{u}_{i,j} + \mathbf{u}_{j,i}) \quad (3c)$$

$$\boldsymbol{\sigma}_{ij} \mathbf{n}_j = \bar{\mathbf{t}}_i \in \Gamma_{\mathbf{t}} \quad (4a)$$

$$\mathbf{u}_i = \bar{\mathbf{u}}_i \in \Gamma_{\mathbf{u}} \quad (4b)$$

$$\Gamma_{\mathbf{t}} \cup \Gamma_{\mathbf{u}} = \partial\Omega \quad \text{and} \quad \Gamma_{\mathbf{t}} \cap \Gamma_{\mathbf{u}} = \emptyset, \quad (4c)$$

where $\boldsymbol{\sigma}$ and $\boldsymbol{\epsilon}$ are the stress and strain tensors, respectively, and \mathbf{u} and \mathbf{b} are the displacement and body force vectors, respectively. The boundary $\partial\Omega$, defined by outward unit normal vector \mathbf{n} , is the union of spaces $\Gamma_{\mathbf{t}}$ and $\Gamma_{\mathbf{u}}$ defining the spaces of prescribed traction, $\bar{\mathbf{t}}$, and displacement, $\bar{\mathbf{u}}$, respectively. The constitutive tensor $\mathbf{C}(\mathbf{x})$ is a function of position due to random spatial fluctuations of the elastic modulus and/or Poisson's ratio of the material occupying Ω . Let a homogenized counterpart of Ω , denoted Ω_H , be occupied by a material with a constitutive tensor, $\bar{\mathbf{C}}$, that is constant within Ω_H but is a function of the displacement boundary conditions (Eq. (4b)), surface tractions (Eq. (4a)), and an integral expression of $\mathbf{C}(\mathbf{x})$. One definition of the effective material properties is that the strain energy in Ω_H equals the strain energy in Ω under the same set of boundary conditions, that is

$$\frac{1}{2} \int_{\Omega_H} \boldsymbol{\epsilon}_0(\mathbf{x}) : \bar{\mathbf{C}} : \boldsymbol{\epsilon}_0(\mathbf{x}) dV = \frac{1}{2} \int_{\Omega} \boldsymbol{\epsilon}(\mathbf{x}) : \mathbf{C}(\mathbf{x}) : \boldsymbol{\epsilon}(\mathbf{x}) dV = \frac{1}{2} \int_{\Gamma_{\mathbf{t}}} \mathbf{u}(\mathbf{x}) \cdot \bar{\mathbf{t}}(\mathbf{x}) d\Gamma_{\mathbf{t}}, \quad (5)$$

where $\boldsymbol{\epsilon}_0(\mathbf{x})$ is the strain in Ω_H , ':' denotes the tensor inner product, and '.' denotes the vector dot product. Note that Eq. (5) is given in the absence of body forces without loss of generality. Consider the case where the Poisson's ratio is approximated as constant and only the elastic modulus $E(\mathbf{x})$ is randomly heterogeneous (the shear modulus $G(\mathbf{x})$ must also therefore be heterogeneous to preserve isotropy). Then the effective elastic modulus, \bar{E} can be factored out of the homogeneous constitutive tensor (i.e. $\bar{\mathbf{C}} = \bar{E}\bar{\mathbf{C}}$), and can be expressed as

$$\bar{E} = \frac{\int_{\Gamma_{\mathbf{t}}} \mathbf{u}(\mathbf{x}) \cdot \bar{\mathbf{t}}(\mathbf{x}) d\Gamma_{\mathbf{t}}}{\int_{\Omega_H} \boldsymbol{\epsilon}_0(\mathbf{x}) : \bar{\mathbf{C}} : \boldsymbol{\epsilon}_0(\mathbf{x}) dV} = \frac{\int_{\Omega} \boldsymbol{\epsilon}(\mathbf{x}) : \mathbf{C}(\mathbf{x}) : \boldsymbol{\epsilon}(\mathbf{x}) dV}{\int_{\Omega_H} \boldsymbol{\epsilon}_0(\mathbf{x}) : \bar{\mathbf{C}} : \boldsymbol{\epsilon}_0(\mathbf{x}) dV}. \quad (6)$$

Similarly, the effective compliance $\bar{D} = \frac{1}{\bar{E}}$ is defined as

$$\bar{D} = \frac{\int_{\Omega_H} \boldsymbol{\epsilon}_0(\mathbf{x}) : \bar{\mathbf{C}} : \boldsymbol{\epsilon}_0(\mathbf{x}) dV}{\int_{\Gamma_{\mathbf{t}}} \mathbf{u}(\mathbf{x}) \cdot \bar{\mathbf{t}}(\mathbf{x}) d\Gamma_{\mathbf{t}}} = \frac{\int_{\Omega_H} \boldsymbol{\epsilon}_0(\mathbf{x}) : \bar{\mathbf{C}} : \boldsymbol{\epsilon}_0(\mathbf{x}) dV}{\int_{\Omega} \boldsymbol{\epsilon}(\mathbf{x}) : \mathbf{C}(\mathbf{x}) : \boldsymbol{\epsilon}(\mathbf{x}) dV}. \quad (7)$$

The effective elastic modulus is bounded by the Reuss (isostress) and Voigt (isostrain) bounds [10]

$$\bar{E}_r \leq \bar{E} \leq \bar{E}_v \quad (8a)$$

$$\text{Reuss: } \bar{E}_r = \frac{1}{V_{\Omega}} \left[\int_{\Omega} E(\mathbf{x})^{-1} dV \right]^{-1} \quad \text{Voigt: } \bar{E}_v = \frac{1}{V_{\Omega}} \int_{\Omega} E(\mathbf{x}) dV \quad (8b)$$

From Eq. (6), the variance of the effective elastic modulus is computed as

$$\text{Var}[\bar{E}] = \frac{1}{C_1^2} \text{Var} \left[\int_{\Gamma_{\mathbf{t}}} \mathbf{u}(\mathbf{x}) \cdot \bar{\mathbf{t}}(\mathbf{x}) d\Gamma_{\mathbf{t}} \right], \quad (9)$$

where $C_1 = \int_{\Omega_H} \boldsymbol{\epsilon}_0(\mathbf{x}) : \bar{\mathbf{C}} : \boldsymbol{\epsilon}_0(\mathbf{x}) dV$. If the random fluctuations of the elastic modulus about its mean value are described by a statistically homogeneous, zero-mean random field, $f(\mathbf{x})$, then the goal of the VRF concept is to establish the following relationship

$$\text{Var}[\bar{E}] = \int_{-\infty}^{\infty} \int_{-\infty}^{\infty} \int_{-\infty}^{\infty} S_f(\kappa_1, \kappa_2, \kappa_3) \text{VRF}_{\bar{E}}(\kappa_1, \kappa_2, \kappa_3) d\kappa_1 d\kappa_2 d\kappa_3, \quad (10)$$

where $S_f(\kappa_1, \kappa_2, \kappa_3)$ is the SDF of $f(\mathbf{x})$. An analogous expression can be established for the effective compliance \bar{D} . The reader is referred to [23,27] for analytically derived expressions for the VRF for the effective flexibility of statically determinate beams.

3. Generalized variability response function (GVRF) methodology

Only for specific cases of statically determinate structures can VRFs be proven to exist because, in general, the displacement cannot be described by a function that is separable with respect to the applied traction and the stochastic parameters in the constitutive law. Therefore, for statically indeterminate structures, the integrand in Eq. (1) cannot be obtained. However, the GVRF methodology generalizes the VRF concept so that it is applicable to statically indeterminate structures. The original work delineating the methodology can be found in Ref. [18] where it is applied to a linear statically indeterminate beam. This methodology is based on the premise that there exists a GVRF for indeterminate structures that is approximately independent of the PDF and/or SDF of the uncertain parameters. The main objective of the methodology is to numerically compute GVRFs for a variety of random field models describing the uncertain parameters and to determine the degree to which the above premise is valid (of PDF/SDF independence). This section extends the methodology to linear continua where the uncertain parameters are modeled by two-dimensional random fields.

3.1. GVRF for problems involving two-dimensional random fields

Consider a specific linear continuum with a randomly heterogeneous material property (e.g. the compliance $D(\mathbf{x})$) modeled by a zero-mean, two-dimensional homogeneous random field $f(\mathbf{x})$, where $\mathbf{x} = (x_1, x_2) \in \mathbb{R}^2$, with SDF $S_f(\kappa_1, \kappa_2)$ and prescribed marginal PDF. The variance of its effective property \bar{D} can be written in the following integral form involving some function $VRF_{\bar{D}_f}(\kappa_1, \kappa_2)$

$$\text{Var}[\bar{D}] = \int_{-\infty}^{\infty} \int_{-\infty}^{\infty} S_f(\kappa_1, \kappa_2) VRF_{\bar{D}_f}(\kappa_1, \kappa_2) d\kappa_1 d\kappa_2. \quad (11)$$

Similarly, the variance of the displacement response $u(\mathbf{x})$ can be written in the following integral form involving some function $VRF_{u_f}(\mathbf{x}, \kappa_1, \kappa_2)$

$$\text{Var}[u(\mathbf{x})] = \int_{-\infty}^{\infty} \int_{-\infty}^{\infty} S_f(\kappa_1, \kappa_2) VRF_{u_f}(\mathbf{x}, \kappa_1, \kappa_2) d\kappa_1 d\kappa_2. \quad (12)$$

The aim of this work is to explore the existence of a function $VRF_D(\kappa_1, \kappa_2)$, that is $VRF_D(\kappa_1, \kappa_2) \approx VRF_{D_f}(\kappa_1, \kappa_2) \forall f$ (similarly, $VRF_u(\mathbf{x}, \kappa_1, \kappa_2) \approx VRF_{u_f}(\mathbf{x}, \kappa_1, \kappa_2) \forall f$). For the sake of conciseness, the methodology is only described below for the displacement response rather than the effective property since the formulation is essentially identical. The left-hand-side of the above equation, $\text{Var}[u(\mathbf{x})]$, can be easily computed through brute-force Monte Carlo simulation by generating sample functions of random field $f(\mathbf{x})$ using its prescribed SDF and PDF. It is obvious, however, that there is no unique solution for $VRF_{u_f}(\mathbf{x}, \kappa_1, \kappa_2)$ in Eq. (12), given $S_f(\kappa_1, \kappa_2)$. Assuming quadrant symmetry [30], Eq. (12) can be written in discretized form as

$$\text{Var}[u(\mathbf{x})] = 4(\Delta\kappa)^2 \sum_{j=1}^N \sum_{l=1}^N S_f(\kappa_j, \kappa_l) VRF_u(\mathbf{x}, \kappa_j, \kappa_l), \quad \kappa_j, \kappa_l \in [0, \kappa_u], \quad (13)$$

where the wave number domain is discretized into $N \times N$ equal intervals $\Delta\kappa$ between 0 and an upper cutoff wave number κ_u , and the set of wave numbers $\{\kappa_j = \frac{j\Delta\kappa}{2}, \kappa_l = \frac{l\Delta\kappa}{2}\}$ are the center points of the intervals. Eq. (13) can also be written equivalently as a dot product between two vectors

$$\text{Var}[u(\mathbf{x})] = 4(\Delta\kappa)^2 \mathbf{S}_q \cdot \mathbf{VRF}_q, \quad (14)$$

where index $q = (j-1) \times N + l$ giving $VRF_q = VRF_u(\mathbf{x}, \kappa_j, \kappa_l)$ and $S_q = S_f(\kappa_j, \kappa_l)$. Consider now that N^2 different SDFs, $S_{f_p}(\kappa_1, \kappa_2)$, $p = 1, 2, \dots, N^2$, are selected (all with the same marginal PDF) and that Eq. (14) is written repeatedly for each one of these N^2 SDFs. This leads to a system of N^2 linear equations with N^2 unknowns, where the unknowns are contained in the vector of discretized values of the VRF (denoted from now on as GVRF and standing for generalized variability response function). The left-hand-side vector of variances can be easily computed by Monte Carlo simulations as mentioned earlier, and the system of linear equations with N^2 unknowns that provides a unique solution for the vector of discretized values of the GVRF is written as

$$\text{Var}[u(\mathbf{x})_p] = 4(\Delta\kappa)^2 \mathbf{S}_{pq} \mathbf{GVRF}_q. \quad (15)$$

Each of the N^2 rows in Eq. (15), identified by index p , corresponds to a different SDF, $S_{f_p}(\kappa_1, \kappa_2)$; $p = 1, 2, \dots, N^2$. The index q is defined as in Eq. (14), and thus the matrix of SDFs \mathbf{S} relates to the individual SDFs as $\mathbf{S}_{pq} = S_{f_p}(\kappa_j, \kappa_l)$ and the vector GVRF is defined as $\mathbf{GVRF}_q = \mathbf{GVRF}(\mathbf{x}, \kappa_j, \kappa_l)$. The choice of the structure of the N^2 SDFs is detailed in Section 3.3.

The entire process resulting in Eq. (15) is repeated for several other sets of N^2 different SDFs paired with a wide range of different marginal PDFs. If the solutions of all these systems of N^2 linear equations yield approximately the same solution for the GVRF (allowing for small differences due to numerical reasons), then it can be claimed that an approximate VRF exists for this structure that is almost entirely independent of the SDF and the PDF of the random field modeling the uncertain system properties.

It is worth noting that the GVRF methodology developed in this paper is capable of handling one random field. Thus, for the problems studied in this paper, only a single component of the isotropic elastic constitutive tensor is modeled as a random field (i.e. the compliance is a random field and Poisson’s ratio is considered to be deterministic). For a more comprehensive representation, the two components of the isotropic elastic constitutive tensor should be modeled as correlated random fields. However, the focus of this paper is to develop the GVRF methodology in two dimensions. Developing the GVRF methodology for multiple, correlated random fields is beyond the scope of this paper and is the subject of future studies.

3.2. Non-Gaussian random fields considered

The non-Gaussian random field models considered are either memoryless translation fields [9] or associated fields [3,4]. The underlying field is denoted by $g(x_1, x_2)$ and the transformed non-Gaussian field by $f(x_1, x_2)$, while the two corresponding marginal cumulative distribution functions (CDFs) are denoted by $F_g(\cdot)$ and $F_f(\cdot)$, respectively. Then, whether $f(x_1, x_2)$ is a translation field or an associated field, it is defined through the following transformation

$$f(x_1, x_2) = F_f^{-1}(F_g(g(x_1, x_2))). \tag{16}$$

When $f(x_1, x_2)$ is a translation field, $g(x_1, x_2)$ is a Gaussian field. When $f(x_1, x_2)$ is an associated field, $g(x_1, x_2)$ is a U-shaped Beta random sinusoid field. The marginal PDFs considered in the following examples for $f(x_1, x_2)$ include truncated Gaussian, Lognormal, and Uniform distributions.

Realizations of $f(x_1, x_2)$ can be generated by simulating $g(x_1, x_2)$ and then performing the transformation in Eq. (16). In the case of a translation field for $f(x_1, x_2)$, the underlying Gaussian field $g(x_1, x_2)$ is simulated using the Spectral Representation Method outlined in [26]. In the case of an associated field for $f(x_1, x_2)$, the underlying U-shaped Beta random field $g(x_1, x_2)$ has a specific SDF which consists of a delta function centered at wave number $(\kappa_{\delta_1}, \kappa_{\delta_2})$, given by

$$S_g(\kappa_1, \kappa_2) = \frac{1}{2} \sigma_g^2 [\delta(\kappa_1 - \kappa_{\delta_1}, \kappa_2 - \kappa_{\delta_2}) + \delta(\kappa_1 + \kappa_{\delta_1}, \kappa_2 + \kappa_{\delta_2})], \tag{17}$$

while the field itself can be expressed as

$$g(x_1, x_2) = \sqrt{2} \sigma_g \cos(\kappa_{\delta_1} x_1 + \kappa_{\delta_2} x_2 + \theta), \quad \theta \text{ Uniform in } [0, 2\pi]. \tag{18}$$

Eq. (18) can be used in a straightforward way to generate sample realizations of $g(x_1, x_2)$.

The non-Gaussian random field $f(x_1, x_2)$ (whether translation or associated) is given by the following expressions for the three marginal PDFs considered.

Truncated Gaussian (TG)

$$f(x_1, x_2) = \begin{cases} a_l, & s\Phi^{-1}(F_g(g(x_1, x_2))) + m < a_l \\ s\Phi^{-1}(F_g(g(x_1, x_2))) + m, & a_l \leq s\Phi^{-1}(F_g(g(x_1, x_2))) + m \leq a_u \\ a_u, & a_u < s\Phi^{-1}(F_g(g(x_1, x_2))) + m. \end{cases} \tag{19}$$

Uniform (UN)

$$f(x_1, x_2) = (a_u - a_l)F_g(g(x_1, x_2)) + a_l. \tag{20}$$

Lognormal (LN)

$$f(x_1, x_2) = \exp\left(m + s\Phi^{-1}(F_g(g(x_1, x_2)))\right) + a_l. \tag{21}$$

The parameters a_l and a_u are the lower and upper bounds of $f(x_1, x_2)$, respectively, and m and s are parameters to shift and scale the underlying random field. One case is considered from each one of the above three probability distributions and the resulting three cases for the marginal PDFs of $f(x_1, x_2)$ are fully defined in Table 1. It should be noted that the parameters have been chosen such that all three of these marginal PDFs have mean values equal to zero.

Table 1
Parameters of three zero-mean marginal PDFs considered for $f(x_1, x_2)$.

PDF	Parameters				σ_f
	a_l	a_u	m	s	
LN	-.799	-	-.45	$\sqrt{.45}$.60
TG	-.90	.90	0.0	1.0	.67
UN	-.99	.99	-	-	.57

The CDFs of the two underlying fields are given by

$$\text{Gaussian : } F_g(g(x_1, x_2)) = \Phi(g(x_1, x_2)) = \int_{-\infty}^{g(x_1, x_2)} \frac{1}{\sqrt{2\pi}} \exp\left(-\frac{s^2}{2}\right) ds, \quad -\infty < g(x_1, x_2) < \infty \tag{22a}$$

$$\begin{aligned} \text{U-Beta : } F_g(g(x_1, x_2)) &= 1 - \frac{1}{\pi} \cos^{-1}\left(\frac{g(x_1, x_2)}{\sqrt{2}}\right) = 1 - \frac{1}{\pi} \cos^{-1}(\cos(\kappa_{\delta_1} x_1 + \kappa_{\delta_2} x_2 + \theta)), \quad -\sqrt{2} < g(x_1, x_2) \\ &< \sqrt{2}. \end{aligned} \tag{22b}$$

Both of the above CDFs have zero mean and unit standard deviation. Note that although (x_1, x_2) appears in the expression for the marginal PDF of the U-beta distribution, it can be shown that the marginal PDF is independent of (x_1, x_2) due to the Uniform distribution of θ and the 2π periodicity of the cosine.

3.3. Families of spectral density functions considered

All the components of the matrix in Eq. (15) involve SDFs of the transformed fields $f_p(x_1, x_2)$; $p = 1, 2, \dots, N^2$. However, it is the underlying fields $g_p(x_1, x_2)$; $p = 1, 2, \dots, N^2$ that are defined first, and then they are transformed into the corresponding $f_p(x_1, x_2)$; $p = 1, 2, \dots, N^2$ through Eq. (16). The criteria for selecting one family of N^2 underlying fields $g_p(x_1, x_2)$; $p = 1, 2, \dots, N^2$ are the following.

1. The SDFs of the N^2 fields $g_p(x_1, x_2)$; $p = 1, 2, \dots, N^2$ should show as high a diversity as possible in providing power over the entire wave number range considered: $[0, \kappa_u] \times [0, \kappa_u]$.
2. All of these N^2 fields should have the same marginal PDF $f_g(\cdot)$ and consequently the same variance.
3. The N^2 SDFs should be organized in a way such that the condition number of the resulting matrix is minimized.

The structure chosen to satisfy the aforementioned criteria is shown in Fig. 1. The SDFs of the N^2 fields $g_p(x_1, x_2)$; $p = 1, 2, \dots, N^2$ all have the same shape, differing only by a shift in the wavenumber domain, which is made in both dimensions (κ_1, κ_2) by increments of $\Delta\kappa$. In order for all N^2 fields to have the same variance, the corresponding SDFs are defined in a circulant manner: as the SDFs are shifted towards the upper cutoff wave number κ_u , the values that would extend beyond κ_u are carried over to the origin of the wave number domain for each dimension as described by Eq. (23). Since the shifting is performed in each dimension of (κ_1, κ_2) , it is necessary to express index p by two indices (m, n) where $p = N(m - 1) + n$. The circulant structure is demonstrated in Fig. 1 where $\kappa_u = 1.2\pi$ and $N = 16$. The SDF of $g_{1,1}(x_1, x_2)$ (out of the N^2 SDFs $S_{g_{m,n}}(\kappa_1, \kappa_2)$; $m = 1, 2, \dots, N$; $n = 1, 2, \dots, N$) is known as the parent SDF of this family and is denoted by $S_p(\kappa)$. This parent SDF is shown in Fig. 1a for one of the cases considered in this study and is denoted by $S_{p1}(\kappa_1, \kappa_2)$ (exponential decay defined in the first row of Eq. (24)). Five more SDFs are shown from this family in Fig. 1: $p = 40$ (i.e. $S_{p13,8}(\kappa_1, \kappa_2)$), $p = 93$ (i.e. $S_{p16,13}(\kappa_1, \kappa_2)$), $p = 120$ (i.e. $S_{p18,8}(\kappa_1, \kappa_2)$), $p = 180$ (i.e. $S_{p12,4}(\kappa_1, \kappa_2)$), and $p = 205$ (i.e. $S_{p13,13}(\kappa_1, \kappa_2)$) (out of a total of 256). The $(m, n)^{th}$ SDF of a family $S_{g_{m,n}}(\kappa_1, \kappa_2)$ is defined in terms of the parent SDF $S_p(\kappa_1, \kappa_2)$ as

$$S_{g_{m,n}}(\kappa_j, \kappa_l) = \begin{cases} S_p(\kappa_j + \kappa_u - m\Delta\kappa + \Delta\kappa, \kappa_l + \kappa_u - n\Delta\kappa + \Delta\kappa), & 0 \leq \kappa_j \leq (m - 1)\Delta\kappa, \quad 0 \leq \kappa_l \leq (n - 1)\Delta\kappa \\ S_p(\kappa_j - m\Delta\kappa, \kappa_l + \kappa_u - n\Delta\kappa + \Delta\kappa), & m\Delta\kappa \leq \kappa_j \leq \kappa_u, \quad 0 \leq \kappa_l \leq (n - 1)\Delta\kappa \\ S_p(\kappa_j + \kappa_u - m\Delta\kappa + \Delta\kappa, \kappa_l - n\Delta\kappa), & 0 \leq \kappa_j \leq (m - 1)\Delta\kappa, \quad n\Delta\kappa \leq \kappa_l \leq \kappa_u \\ S_p(\kappa_j - m\Delta\kappa, \kappa_l - n\Delta\kappa), & m\Delta\kappa \leq \kappa_j \leq \kappa_u, \quad n\Delta\kappa \leq \kappa_l \leq \kappa_u \end{cases} \tag{23}$$

for $(\kappa_1, \kappa_2) \in [0, \kappa_u] \times [0, \kappa_u]$ and is symmetric about $\kappa_2 = 0$ (i.e. $S_{g_{m,n}}(\kappa_1, \kappa_2) = S_{g_{m,n}}(\kappa_1, -\kappa_2)$).

Two families of N^2 SDFs are considered in this study. The corresponding parent SDFs are denoted by $S_{p1}(\kappa_1, \kappa_2)$ and $S_{p2}(\kappa_1, \kappa_2)$ and are given by

$$S_{p1}(\kappa_1, \kappa_2) = \frac{2}{\pi} \exp(-2(\kappa_1^2 + \kappa_2^2)) S_{p2}(\kappa_1, \kappa_2) = \delta(\kappa_1, \kappa_2). \tag{24}$$

It should be noted that $S_{p2}(\kappa_1, \kappa_2)$ is used for the underlying U-shaped Beta random sinusoid field, while $S_{p1}(\kappa_1, \kappa_2)$ is used for the underlying Gaussian field.

The preceding discussion described the definition of a family of N^2 underlying fields $g_p(x_1, x_2)$; $p = 1, 2, \dots, N^2$ and of their corresponding SDFs. The ultimate objective is to determine the spectral functions of the transformed fields $f_p(x_1, x_2)$; $p = 1, 2, \dots, N^2$ so that they can be used to construct the matrix in Eq. (15). The SDFs of $f_p(x_1, x_2)$; $p = 1, 2, \dots, N^2$ can be computed numerically in a straightforward way using translation field theory [9] or associated field theory [17].

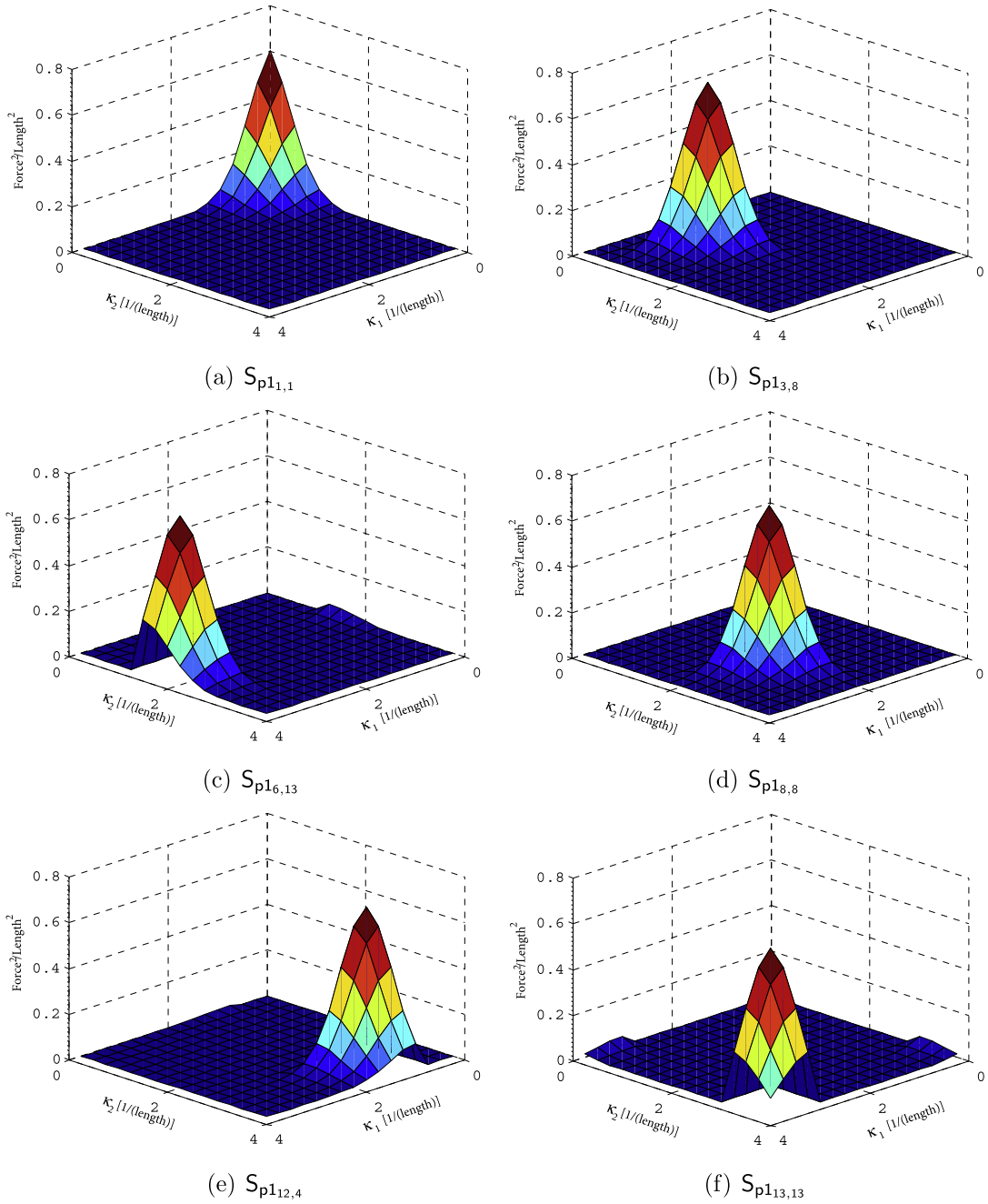


Fig. 1. Selected members of a family of SDFs of an underlying Gaussian field. The parent SDF for this family is shown in (a) and is defined in the first row of Eq. (24).

It is important to note that the structure of the matrix of SDFs in Eq. (15) is a direct extension from the concept of the GVRM methodology for one-dimensional stochasticity. For two-dimensional problems, this matrix has an unavoidably high condition number making it difficult to accurately solve the system of linear equations in Eq. (15) through matrix inversion or direct solving. For example, the condition number for the matrix associated with the family of SDFs S_{p1} in Eq. (24) having the Lognormal marginal PDF (LN) in Table 1 is

$$\|S\|_2 \times \|S^{-1}\|_2 = 676.8, \tag{25}$$

where the size of the matrix is 256×256 , and $\|\cdot\|_2$ is the ℓ^2 norm (this is compared to a condition number of approximately 19.0 for a family of SDFs associated with one-dimensional Lognormal translation fields). However, by taking advantage of the fact that VRFs are by definition non-negative, Eq. (15) can be solved using a non-negative least squares algorithm (NNLS), that is

$$\text{Minimize } \|4(\Delta\kappa)^2 \mathbf{S} \cdot \text{GVRF} - \text{Var}[u]\| \text{ for } \text{GVRF} \geq 0. \quad (26)$$

The MATLAB routine 'LSQNONNEG' was utilized for this purpose. Its implementation follows the algorithm in Ref. [15, Chapter 23, Section 3], which contains proofs regarding convergence (i.e. proof of reaching the Karush–Kuhn–Tucker condition necessary for an optimal solution vector and thus the finite convergence of the algorithm) and techniques to overcome finite numerical precision. Additional numerical and computational challenges are involved in extending the GVRF formulation from one dimension to two dimensions. There is an increase in computational costs due to slower convergence of response statistics, as well as requiring N^2 random fields (as opposed to N random fields). Also, establishing the matrix of SDFs requires an inverse Fourier transform of the underlying SDF to its autocorrelation, a transformation of the underlying autocorrelation to the autocorrelation of the mapped field, and a Fourier transform to get the SDF of the mapped field. There are numerical precision concerns associated with these numerical operations which are more challenging, although not insurmountable, for two-dimensional fields than one-dimensional fields.

3.4. A note on computational demand

It should be noted that the GVRF methodology is computationally intensive. Within each family (defined through a parent SDF and a marginal PDF), each of the N^2 random fields $f_p(x_1, x_2)$; $p = 1, 2, \dots, N^2$ requires a set of Monte Carlo simulations to determine a variance on the left-hand-side of Eq. (15). These intensive computations are performed on a IBM Blue Gene supercomputer owned by Brookhaven National Laboratory using the IBM Fortran90 XL compiler. Each set of Monte Carlo simulations involves 102,400 deterministic runs that are distributed over 4096 processors for a total of about 2 h of CPU time for all N^2 sets of Monte Carlo simulations for a given family of random fields.

It is noted that the GVRF methodology is essentially a brute-force procedure to explore the SDF/PDF independence of variability response functions for certain classes of structures. Once this independence is established, the GVRF for any structure in this class can be determined by considering just one family of N^2 random fields. Furthermore, once the GVRF is established for a structure, the variance of its response can be computed for any statistically homogeneous random field describing the uncertain system properties with minimal computational effort (a simple integration of the type shown in Eq. (12)). The initial upfront expense of the GVRF methodology becomes worthwhile if a large number of random fields are to be examined or especially if a sensitivity analysis is needed (there is no other way currently available to perform a full sensitivity analysis with respect to spectral properties).

4. Numerical examples

The performance of the GVRF methodology is studied through two numerical examples involving a linear elastic plane stress structure. The terminology used to identify a family of random fields $f_p(x_1, x_2)$; $p = 1, 2, \dots, N^2$ associated with the computation of a GVRF is explained through the following representative example: S1UN refers to the family of SDFs with parent SDF $S_{p1}(\kappa_1, \kappa_2)$ defined in Eq. (24) and with UN being the Uniform marginal PDF defined in Table 1.

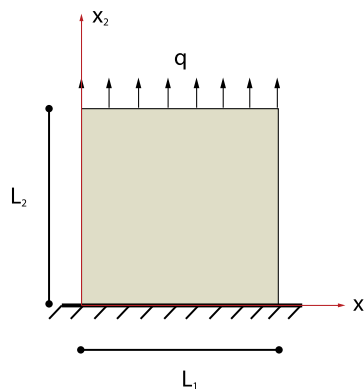


Fig. 2. Plane stress structure analyzed.

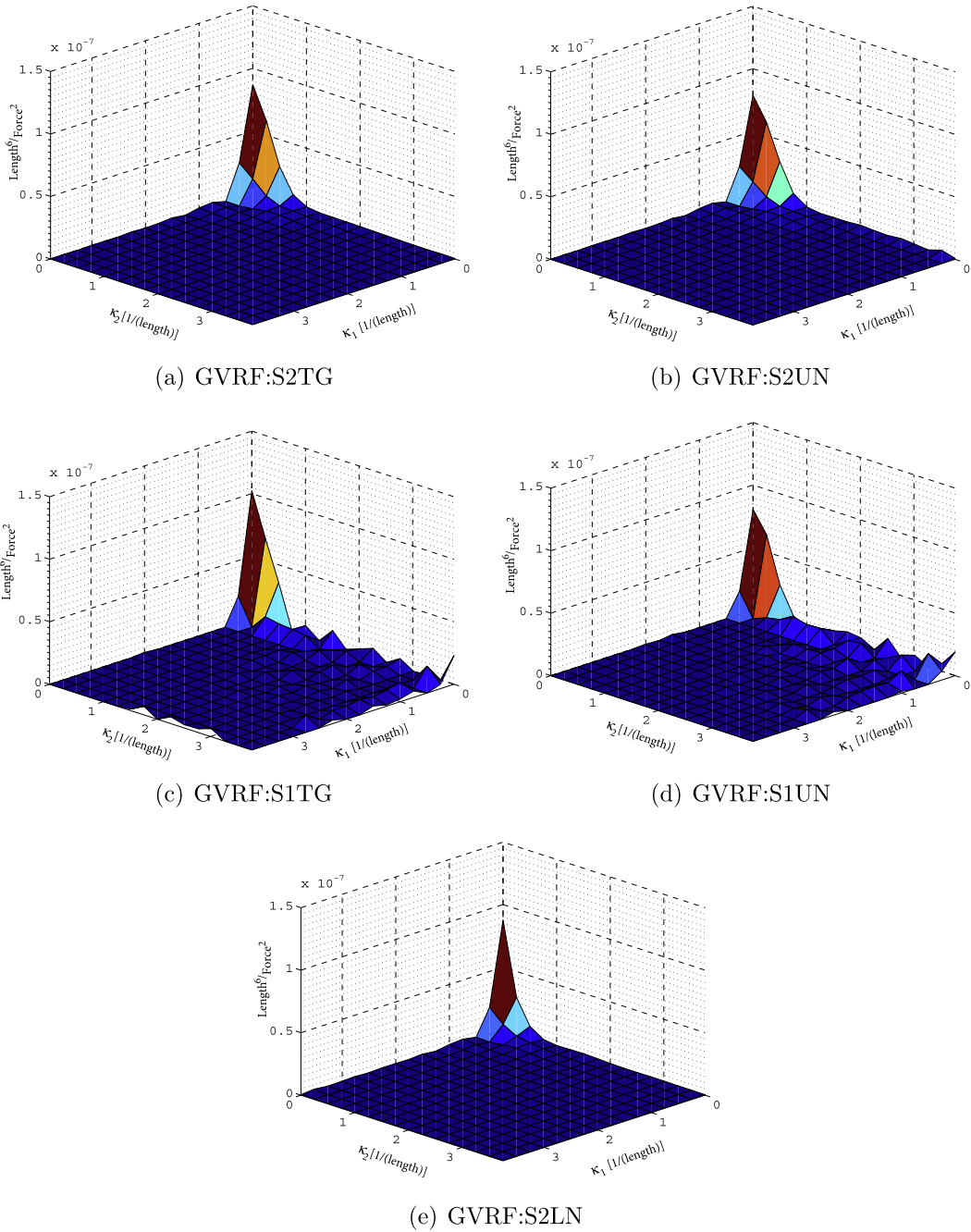


Fig. 3. Computed GVRFs for displacement response at $(L_1/2, L_2)$ for structure in Fig. 2.

4.1. GVRFs for displacement response of a plane stress structure

GVRFs are computed for the displacement response $u(\frac{L_1}{2}, L_2)$ of the structure shown in Fig. 2 with $L_1 = 10$, $L_2 = 10$, $q = 100$, and thickness equal to 1. The heterogeneous compliance (rather than the elastic modulus) is explicitly modeled as a random field in the following way

$$\frac{1}{E(x, y)} = \frac{1 + f(x, y)}{E_0}, \tag{27}$$

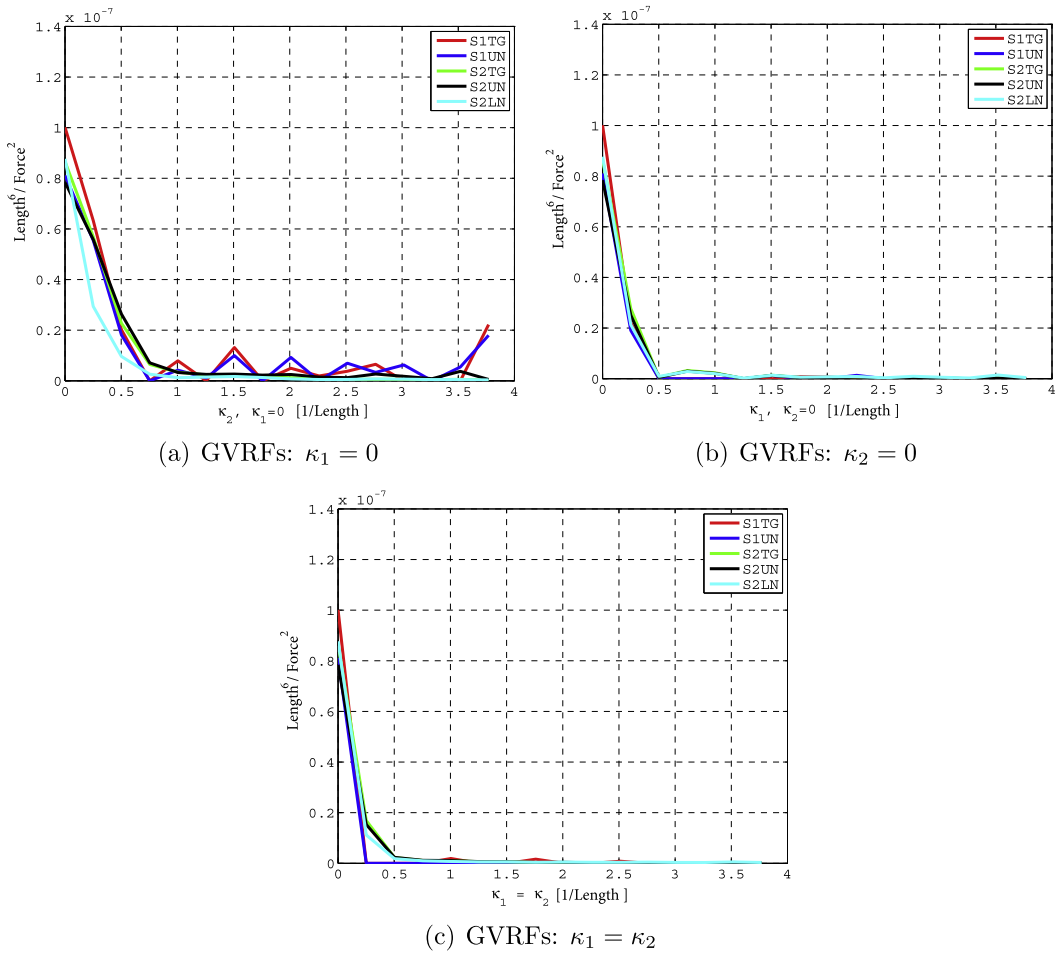


Fig. 4. GVRFs of Fig. 3 at various section cuts.

where the mean compliance is $\frac{1}{E_0} = 8 \times 10^{-8}$ and $f(x, y)$ is a zero-mean statistically homogeneous random field modeling the fluctuations of the compliance about its mean value. Note that since the problem is linear, it is taken to be unitless without loss of generality given that the thin plate kinematics hold.

The GVRFs are plotted in Fig. 3, and they are quite similar for different combinations of SDFs and PDFs. The GVRFs in Fig. 3 are plotted in Fig. 4 at selected section cuts in order to better visualize the discrepancies amongst the various GVRFs. They are plotted along cuts $\kappa_1 = 0$, $\kappa_2 = 0$, and $\kappa_1 = \kappa_2$.

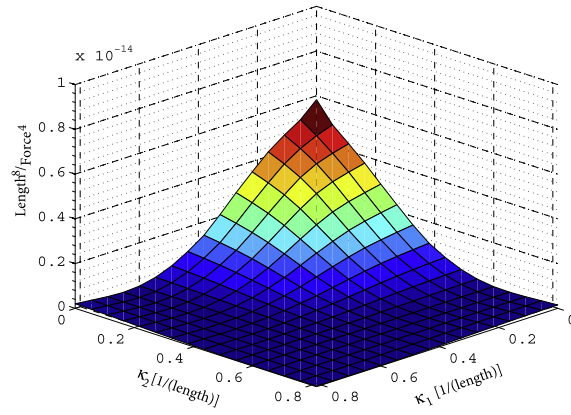
4.2. GVRFs for effective compliance of a plane stress structure

GVRFs are computed for the effective compliance \bar{D} of the plane stress structure analyzed in Section 4.1. For each deterministic analysis in the Monte Carlo simulations, the effective compliance is computed via Eq. (7). GVRFs are plotted for three different marginal PDFs and for SDF family $S_{p2}(\kappa_1, \kappa_2)$ in Fig. 5. Results involving SDF family $S_{p1}(\kappa_1, \kappa_2)$ are not shown for reasons discussed in Section 4.4. Instead, the SDF independence is demonstrated by the validation procedure described in Section 4.3.

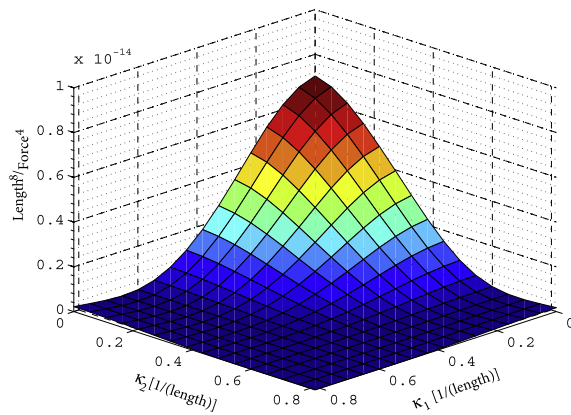
The GVRFs in Fig. 5 are plotted in Fig. 6 at selected section cuts in order to better visualize the discrepancies amongst the various GVRFs. They are plotted along cuts $\kappa_1 = 0$, $\kappa_2 = 0$, and $\kappa_1 = \kappa_2$.

4.3. Validation of GVRFs

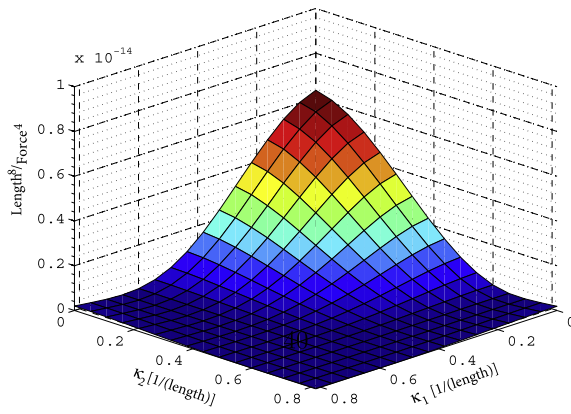
The validity of the GVRFs is tested by computing the coefficient of variation (COV) of the displacement response and effective flexibility by Monte Carlo simulation for a different random field model than what was used to determine the GVRFs, and then comparing these results to the predicted COVs determined by the GVRFs. For the first example in Section 4.1,



(a) S2LN



(b) S2TG



(c) S2UN

Fig. 5. GVRFs for effective compliance for plane stress structure in Fig. 2.

the new random field model chosen is a translation field whose marginal PDF is the Lognormal described in Table 1 and whose non-Gaussian SDF is determined from its underlying Gaussian SDF, which is

$$S3(\kappa_1, \kappa_2) = \frac{1}{1.045} \exp(-3(\kappa_1^2 + \kappa_2^2)), \tag{28}$$

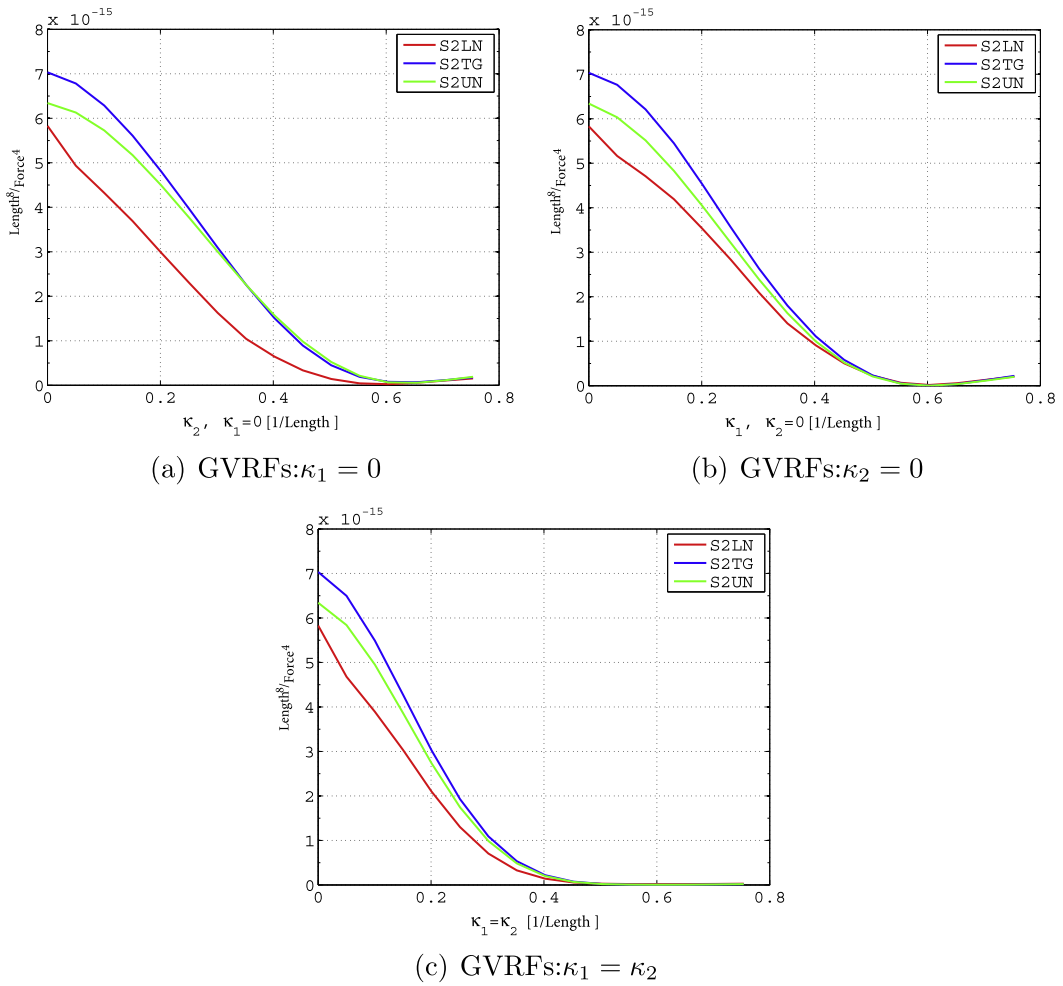


Fig. 6. Computed GVRFs of Fig. 5 at various section cuts.

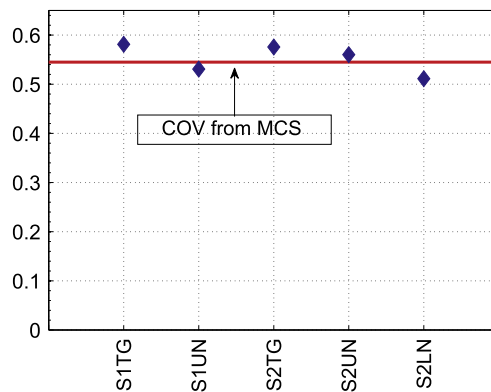


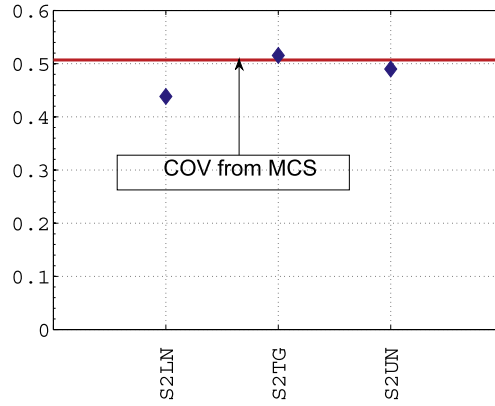
Fig. 7. Validation results for example in Section 4.1: the red line indicates the exact COV of the response displacement determined by brute force Monte Carlo simulation using $S3(\kappa_1, \kappa_2)$ in Eq. (28) and the Lognormal PDF in Table 1. The blue diamonds are the predicted COVs by the GVRFs using Eqs. (30) and (32) and the translated $S3(\kappa_1, \kappa_2)$. (For interpretation of the references to color in this figure legend, the reader is referred to the web version of this article.)

where the coefficient $\frac{1}{1.045}$ restrains the underlying Gaussian field to have unit variance. For the example in Section 4.2, three new translation random field models are chosen having the Lognormal, truncated Gaussian, and Uniform marginal PDFs described in Table 1 and non-Gaussian SDFs determined from their underlying Gaussian SDF, which is

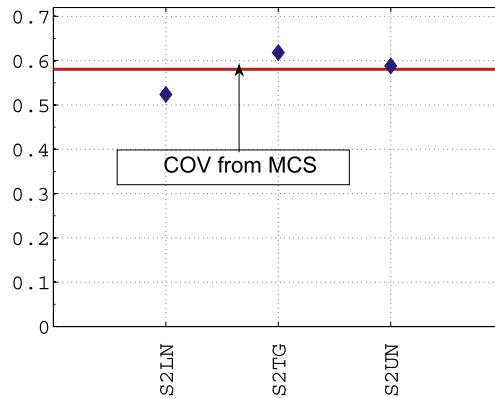
$$S4(\kappa_1, \kappa_2) = 12.626 \exp(-40(\kappa_1^2 + \kappa_2^2)), \tag{29}$$

where the coefficient 12.626 restrains the underlying Gaussian field to have unit variance. The predicted COVs from the GVRFs are determined by performing the integrations shown in Eqs. (30) and (31) to determine the variance and then computing the COV using the mean values stored from the performed Monte Carlo simulations. The variance is given by

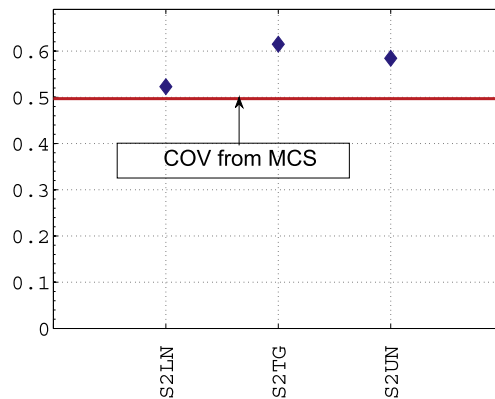
$$\text{Var} \left[u \left(\frac{L_1}{2}, L_2 \right) \right] = \int_{-\kappa_u}^{\kappa_u} \int_{-\kappa_u}^{\kappa_u} S_f(\kappa_1, \kappa_2) GVRF_u \left(\frac{L_1}{2}, L_2, \kappa_1, \kappa_2 \right) d\kappa_1 d\kappa_2 \quad (30)$$



(a) LN



(b) TG



(c) UN

Fig. 8. Validation results for example in Section 4.2: the red lines indicate the exact COVs of the effective compliance through brute force Monte Carlo simulation using $S4(\kappa_1, \kappa_2)$ in Eq. (29) and the Lognormal marginal PDF in Table 1(a), the truncated Gaussian marginal PDF in Table 1(b), and the Uniform marginal PDF in Table 1(c). The blue diamonds are the predicted COVs by the GVRFs using Eqs. (31) and (33) and the translated $S4(\kappa_1, \kappa_2)$ according to the three marginal PDFs. (For interpretation of the references to color in this figure legend, the reader is referred to the web version of this article.)

for the displacement response, and by

$$\text{Var}[\bar{D}] = \int_{-\kappa_u}^{\kappa_u} \int_{-\kappa_u}^{\kappa_u} S_f(\kappa_1, \kappa_2) \text{GVRF}_D(\kappa_1, \kappa_2) d\kappa_1 d\kappa_2 \tag{31}$$

for the effective compliance. In each case, $S_f(\kappa_1, \kappa_2)$ is the SDF of the translated non-Gaussian field obtained from the underlying Gaussian field having SDF $S3(\kappa_1, \kappa_2)$ for the first example and SDF $S4(\kappa_1, \kappa_2)$ for the second example. Solving for the COV yields

$$\text{COV} = \frac{\sqrt{\text{Var}[u(L_1/2, L_2)]}}{|\mathbb{E}[u(L_1/2, L_2)]|} \tag{32}$$

for the displacement response and

$$\text{COV} = \frac{\sqrt{\text{Var}[\bar{D}]}}{|\mathbb{E}[\bar{D}]|} \tag{33}$$

for the effective compliance. Fig. 7 plots the results of the validation for Example 1 and Fig. 8 plots the results of the three validation tests for Example 2. Red lines represent the COVs computed through brute force Monte Carlo simulation using the aforementioned translation field models. The blue diamonds are the COVs predicted by each GVRF using Eqs. (30) and (32) for the first example and Eqs. (31) and (33) for the second example, along with the translated $S3(\kappa_1, \kappa_2)$ (first example) and translated $S4(\kappa_1, \kappa_2)$ (second example).

4.4. Discussion of results

The GVRF methodology performs differently for displacement response than for effective compliance. The GVRFs for the displacement response contain relatively small discrepancies which appear to be significantly due to numerical errors result-

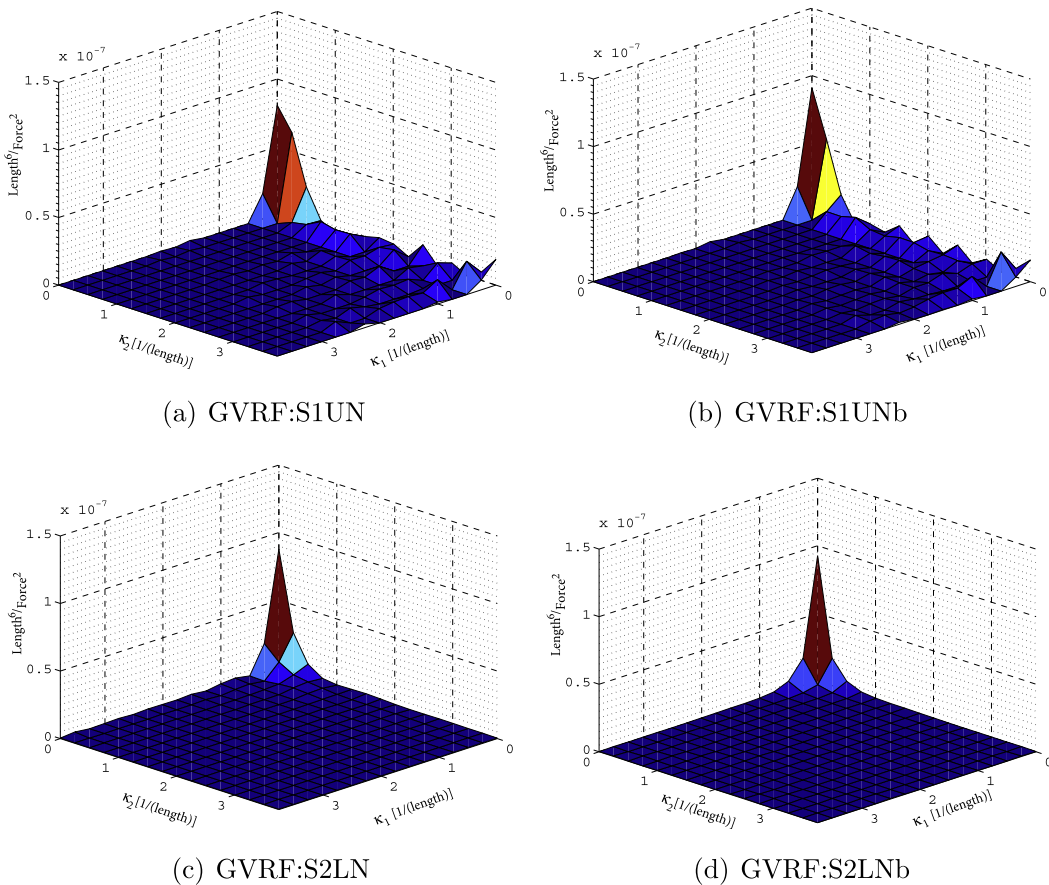


Fig. 9. Comparing GVRFs for displacement response at $(L_1/2, L_2)$ for structure in Fig. 2 using very large variances. GVRF S1UNb refers to a Uniform marginal PDF with variance $\sigma_j^2 = 1.32$ and GVRF S2LNb refers to a Lognormal marginal PDF with variance $\sigma_j^2 = 1.75$.

ing from the discretization of the wavenumber domain and the condition number of the SDF matrix \mathbf{S} . These two sources of numerical errors have opposing effects: as the wavenumber domain is further refined, the size of matrix \mathbf{S} increases as well as its condition number. Matrix \mathbf{S} for SDF family $S_{p2}(\kappa_1, \kappa_2)$ is much better conditioned than for SDF family $S_{p1}(\kappa_1, \kappa_2)$. SDFs of $S_{p2}(\kappa_1, \kappa_2)$ are close to delta functions at different wavenumbers and thus produce a system of equations more linearly independent than SDFs from $S_{p1}(\kappa_1, \kappa_2)$, which have power that is broadly distributed. This explains why GVRFs computed from $S_{p1}(\kappa_1, \kappa_2)$ display numerical noise that is not present in GVRFs from $S_{p2}(\kappa_1, \kappa_2)$ (i.e. see Figs. 3 and 4). Further, the GVRF computed via the Lognormal PDF for SDF family $S_{p1}(\kappa_1, \kappa_2)$ contains too much numerical error and is not shown. The validation exercise of Section 4.3 addresses specifically this issue by comparing predicted response COVs using the computed GVRFs to the results of a Monte Carlo simulation involving a Lognormal random field. As seen in Fig. 7, the comparisons are fairly

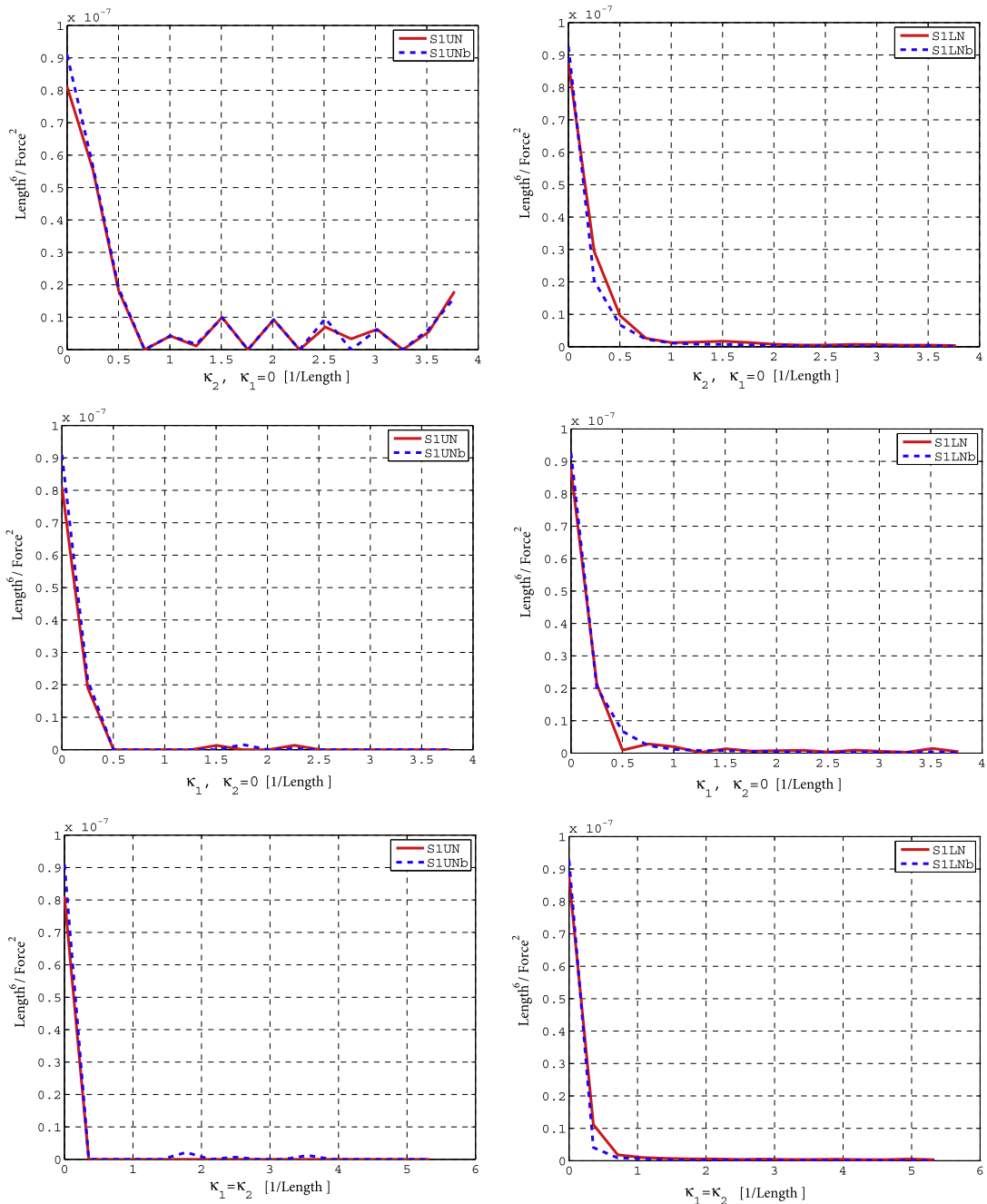


Fig. 10. Comparing GVRFs for displacement response at $(L_1/2, L_2)$ for structure in Fig. 2 using very large variances. GVRFs of Fig. 9 at various section cuts.

accurate, suggesting that GVRFs computed using a Lognormal distribution would be similar to the other GVRFs if the system of equations were better conditioned.

In order to demonstrate that the discrepancies of the GVRFs are mainly due to numerical errors and not PDF dependence, additional GVRFs are computed using the following random fields with very large variances: a Lognormal marginal PDF having SDF family S_{p2} with variance $\sigma_f^2 = 1.75$ (the parameters are $m = -.51$, $s = 1.0$, $a_l = -.9905$ and the corresponding GVRF is denoted as S2LNb), and a Uniform marginal PDF having SDF family S_{p1} with variance $\sigma_f^2 = 1.32$ (the parameters are $a_l = -1.99$, $a_u = 1.99$ and the corresponding GVRF is denoted S1UNb). If there is a PDF dependence on the GVRFs, then the discrepancies will increase as the variances of the random fields increase. Figs. 9 and 10 show these GVRFs are nearly identical with the GVRFs based on the corresponding random fields with smaller variances, implying that any PDF dependence is not significant.

The GVRFs for the effective compliance do not perform as well as those for the displacement response. The degree of dependence of the GVRFs on the PDFs can be observed through those computed via $S_{p2}(\kappa_1, \kappa_2)$ (Figs. (5) and (6)). The shapes of the GVRFs are similar but differ almost by a constant scale factor, as can be seen in Fig. 6. GVRFs computed using SDF family $S_{p1}(\kappa_1, \kappa_2)$ are dominated by the numerical errors discussed above and produce results that are too noisy to be useful. The degree of dependence of the GVRFs on the SDFs is demonstrated through the validation exercises. Here, the three GVRFs computed from $S_{p2}(\kappa_1, \kappa_2)$ are used to predict the COV of the effective compliance resulting from random fields with a completely different SDF. As seen in Fig. (8), the predictions perform reasonably well in general, but in a few cases they contain significant errors (roughly 20 % error for the S2TG GVRF's prediction of Monte Carlo results of random field S4UN).

It is worth noting that it is easier to consider very large variations in the elastic modulus by directly treating the compliance as a random field as done in this work. For example, the compliance modeled using a Uniform distribution with $\sigma_f = .57$ has a corresponding elastic modulus with coefficient of variation equal to 2.45. This is an extremely large variation in the elastic modulus. Due to the one-to-one relation between elastic modulus and compliance, there is no loss of generality to determining the GVRFs of the compliance because one can easily convert the random field model for elastic modulus to one for compliance and vice versa. Therefore, for some practical problems of interest, the variability range will be less than that considered in this work and the PDF/SDF dependence of the GVRFs for effective properties will be less significant.

Nonetheless, it is recognized that the poor conditioning of the system of equations to compute the GVRFs makes it difficult to discern the contributions from each source of discrepancy. These numerical examples demonstrate that the applicability of the GVRF methodology for general continua is promising, but future work must address the critical issue of the numerical conditioning of Eq. (15), such as applying matrix preconditioners, advanced least-squares or optimization algorithms, and alternative structuring of the family of SDFs.

5. Conclusions

The main finding of this paper is that the GVRF methodology can be formulated and successfully applied to structures whose stochasticity is modeled by two-dimensional random fields. This significantly extends the applicability of the GVRF concept, which, prior to this, has only been applied to problems involving one-dimensional random fields. In two numerical examples, GVRFs have been computed for the displacement response as well as the effective compliance of a plane stress structure whose elastic modulus is modeled by a homogeneous two-dimensional random field. The computed GVRFs contain differences (in some cases not insignificant), mainly due to numerical errors for the GVRFs for displacement response and a combination of numerical errors and PDF dependence for GVRFs for effective compliances, as discussed in detail in Section 4.4. However, in general, all the GVRFs exhibit remarkably similar behavior and mostly demonstrate reasonable results in the validation exercises shown in Section 4.3. One of the implications of these results is that the VRF concept has the potential to be a useful technique to quantify the uncertainty of computed effective material properties due to length scale effects. It is a well known issue in multi-scale finite element methods that the computed solution is dependent on the size of the elements and RVE chosen, yet there is no robust way to compute the uncertainty in the solution due to this scale dependence. The work presented in this paper is a step towards developing a robust technique based on the VRF concept to attain such goals.

Acknowledgments

This work was supported by the National Science Foundation under Grant No. CMMI-0928129 with Dr. Mahendra P. Singh and Dr. Kishor Mehta as Program Directors.

References

- [1] C.G. Bucher, M. Shinozuka, Structural response variability-II, *J. Eng. Mech. – ASCE* 114 (12) (1988) 2035–2054.
- [2] D.C. Charnpis, G.I. Schueller, M.F. Pellissetti, The need for linking micromechanics of materials with stochastic finite elements: a challenge for materials science, *Comput. Mater. Sci.* 41 (1) (2007) 27–37.
- [3] G. Deodatis, L. Graham-Brady, R. Micaletti, A hierarchy of upper bounds on the response of stochastic systems with large variation of their properties: random field case, *Probab. Eng. Mech.* 18 (4) (2003) 365–375.
- [4] G. Deodatis, L. Graham-Brady, R. Micaletti, A hierarchy of upper bounds on the response of stochastic systems with large variation of their properties: random variable case, *Probab. Eng. Mech.* 18 (4) (2003) 349–363.

- [5] G. Deodatis, M. Shinozuka, Bounds on response variability of stochastic systems, *J. Eng. Mech. – ASCE* 115 (11) (1989) 2543–2563.
- [6] L. Graham, G. Deodatis, Variability response functions for stochastic plate bending problems, *Struct. Saf.* 20 (2) (1998) 167–188.
- [7] L.L. Graham, G. Deodatis, Response and eigenvalue analysis of stochastic finite element systems with multiple correlated material and geometric properties, *Probab. Eng. Mech.* 16 (1) (2001) 11–29.
- [8] L. Graham-Brady, Statistical characterization of meso-scale uniaxial compressive strength in brittle materials with randomly occurring flaws, *Int. J. Solids Struct.* 47 (18–19) (2010) 2398–2413.
- [9] M. Grigoriu, *Applied Non-Gaussian Processes*, PTR Prentice Hall, 1995.
- [10] R. Hill, The elastic behaviour of a crystalline aggregate, *Proc. Phys. Soc. Sec. A* 65 (1952) 345.
- [11] L. Huyse, M.A. Maes, Random field modeling of elastic properties using homogenization, *J. Eng. Mech.* 127 (1) (2001) 27–36.
- [12] T. Kanit, S. Forest, I. Galliet, V. Mounoury, D. Jeulin, Determination of the size of the representative volume element for random composites: statistical and numerical approach, *Int. J. Solids Struct.* 40 (13–14) (2003) 3647–3679.
- [13] Z.F. Khisaeva, M. Ostoja-Starzewski, On the size of RVE in finite elasticity of random composites, *J. Elast.* 85 (2) (2006) 153–173.
- [14] P.S. Koutsourelakis, Stochastic upscaling in solid mechanics: an exercise in machine learning, *J. Comput. Phys.* 226 (1) (2007) 301–325.
- [15] C.L. Lawson, R.J. Hanson, *Solving Least Squares Problems*, vol. 161, Prentice-hall, Englewood Cliffs, NJ, 1974.
- [16] J.A. Ma, I. Temizer, P. Wriggers, Random homogenization analysis in linear elasticity based on analytical bounds and estimates, *Int. J. Solids Struct.* 48 (2) (2011) 280–291.
- [17] M. Miranda, *On the reponse variability of beam structures with stochastic variations of parameters* (Ph.D. thesis), Columbia University, 2009.
- [18] M. Miranda, G. Deodatis, Generalized variability response functions for beam structures with stochastic parameters, *J. Eng. Mech.* 138 (9) (2012) 1165–1185.
- [19] H.C. Noh, H.G. Kwak, Response variability due to randomness in Poisson's ratio for plane-strain and plane-stress states, *Int. J. Solids Struct.* 43 (5) (2006) 1093–1116.
- [20] V. Papadopoulos, G. Deodatis, Response variability of stochastic frame structures using evolutionary field theory, *Comput. Methods Appl. Mech. Eng.* 195 (9–12) (2006) 1050–1074.
- [21] V. Papadopoulos, M. Papadrakakis, G. Deodatis, Analysis of mean and mean square response of general linear stochastic finite element systems, *Comput. Methods Appl. Mech. Eng.* 195 (41–43) (2006) 5454–5471.
- [22] K. Sab, On the homogenization and the simulation of random materials, *Eur. J. Mech. A-Solids* 11 (5) (1992) 585–607.
- [23] G.D. Sanjay Arwarde, Variability response functions for effective properties, *Probab. Eng. Mech.* 26 (2011) 174–181.
- [24] M. Shinozuka, Structural response variability, *J. Eng. Mech. – ASCE* 113 (6) (1987) 825–842.
- [25] M. Shinozuka, G. Deodatis, Response variability of stochastic finite-element systems, *J. Eng. Mech. – ASCE* 114 (3) (1988) 499–519.
- [26] M. Shinozuka, G. Deodatis, Simulation of stochastic processes by spectral representation, *Appl. Mech. Rev.* 44 (4) (1991) 191–204.
- [27] K. Teferra, S.R. Arwade, G. Deodatis, Stochastic variability of effective properties via the generalized variability response function, *Comput. Struct.* 110–111 (2012) 107–115.
- [28] K. Teferra, G. Deodatis, Variability response functions for beams with nonlinear constitutive laws, *Probab. Eng. Mech.* 29 (2012) 139–148.
- [29] K. Terada, M. Hori, T. Kyoya, N. Kikuchi, Simulation of the multi-scale convergence in computational homogenization approaches, *Int. J. Solids Struct.* 37 (16) (2000) 2285–2311.
- [30] E. Vanmarcke, *Random Fields: Analysis and Synthesis*, The MIT Press, 1983.
- [31] F.J. Wall, G. Deodatis, Variability response functions of stochastic plane-stress strain problems, *J. Eng. Mech. – ASCE* 120 (9) (1994) 1963–1982.
- [32] X.F. Xu, L. Graham-Brady, A stochastic computational method for evaluation of global and local behavior of random elastic media, *Comput. Methods Appl. Mech. Eng.* 194 (42–44) (2005) 4362–4385.